**Rare Metal Materials and Engineering**
Volume 52, Issue 3, March 2023
Available online at www.rmme.ac.cn

Science Press

**Cite this article as**: Wu Guodong, Shen Jingfang, Zhang Wenjing, et al. Numerical Simulation of Residual Stress and Deformation of TC4 Thin-Walled Parts During Argon Arc Welding[J]. Rare Metal Materials and Engineering, 2023, 52(03): 798-805.

ARTICLE

# Numerical Simulation of Residual Stress and Deformation of TC4 Thin-Walled Parts During Argon Arc Welding

**Wu Guodong[1], Shen Jingfang[2], Zhang Wenjing[2], Xie Shaopeng[1], Fang Zhizhong[3], Huang Xiaoa[1]**

*[1] Guangdong University of Technology, Jieyang 522000, China; [2] Guangdong Technion Israel Institute of Technology, Shantou 515063, China; [3] AECC Guizhou Liyang Aviation Power Co., Ltd, Guiyang 550000, China*

**Abstract:** The transient method was used to simulate the argon arc welding process of large-scale thin-walled parts with multiple welds of TC4 alloy as aeroengine based on the SYSWELD professional welding simulation software. The influence of the welding line energy, fixture constraint state, and welding sequence on welding temperature field, welding deformation, and residual stress was analyzed. Results show that the welding deformation is increased exponentially with increasing the line energy, and the optimal line energy for argon arc welding is 310 J/mm. The application of welding fixture constraint can effectively reduce the welding deformation, but causes in the larger welding residual stress and wider distribution area. The decentralized symmetric welding can reduce the overall welding deformation of parts with multiple welds.

**Key words:** TC4; numerical simulation; argon arc welding

With their high specific strength and excellent corrosion resistance, the lightweight titanium alloys have been widely used to replace the steel and superalloy in the aerospace field. Thus, the thrust-to-weight ratio of aeroengines is significantly improved by the application of titanium alloys[1–4]. TC4 alloy is commonly used for large-scale thin-walled parts of aeroengine, but the insufficient rigidity, sizeable residual stress, severe deformation after welding, and welding cracks restrict its application. Moreover, under the conditions of high temperature, high speed, and high vibration, the thin-walled parts are prone to brittleness or fatigue fracture under the continuous operation of aeroengine due to the weld defects and residual stress, thereby resulting in the failure[5–9]. Since titanium alloys are relatively expensive, the high cost and long cycle time for investigation of welded titanium alloys restrict their welding experiments. Thus, the simulation of welding process is proposed, which can significantly reduce the experiment cost and shorten the experiment period.

Extensive researches have been made on welding simulation[10–13]. Among all the simulation softwares, SYSWELD software can realize the coupling calculation of machinery, heat conduction, and metal metallurgy, which is widely used in welding simulation. Saravanan et al[11] reported the effect of different welding parameters on the temperature distribution and hardness distribution in Hastelloy C-276 laser-welded joints, and confirmed that SYSWELD software is suitable to predict the weld profile and temperature distribution. Hemmesi et al[14] simulated the welding process of structural S355J2H steel by SYSWELD, and investigated the effect of residual welding stress on the fatigue life of steel tubular joints. Shiraiwa et al[15] developed a new fatigue prediction method for welded structures by combining SYSWELD calcualtion, thermomechanical finite element method, crystal plasticity model, and extended finite element method. Liu et al[16] conducted a welding stress analysis on the aircraft engine mounting frame based on SYSWELD software. Xiong et al[17] optimized the welding parameters of the rear frame of the electric pallet forklift by SYSWELD software, which reduced the maximum welding deformation by 12.2%. However, in the aeroengine field, the welding simulation of larger-scale thin-walled and multi-welded parts is rarely reported[18].

In this research, the welding process of large-scale thin-

Received date: August 18, 2022
Foundation item: Guangdong Province Science and Technology Special Fund Project (STKJ 2021180, STKJ 2021184)
Corresponding author: Shen Jingfang, Master, Guangdong Technion Israel Institute of Technology, Shantou 515063, P. R. China, Tel: 0086-754-88077154, E-mail: jingfang.shen@gtiit.edu.cn

walled multi-welded part of TC4 alloy used for aeroengines was simulated by the SYSWELD software. The transient simulation calculation method was adopted, which was a suitable and accurate method under the condition of weld length<3 m[19–22]. The simulation process included CAD modeling, heat source selection, mesh division, and process parameter optimization. The effects of welding line energy, welding sequence, and fixture constraint state on the welding temperature field, stress field, and deformation distribution were analyzed. The part deformation and residual stress distribution area after welding could be predicted based on the simulation results. This research provided a theoretical basis for optimization of fixture design, welding sequence, and welding parameters.

## 1 Part Structure

The material selected in this simulation was TC4 alloy, and its composition is listed in Table 1. TC4 alloy with medium strength is composed of the $\alpha+\beta$ dual-phase structure, which contains 6wt% $\alpha$-stabilizing element Al and 4wt% $\beta$-stabilizing element V. The melting temperature range of TC4 alloy is 1630–1650 °C, and the linear expansion coefficient at 20 °C is $9.1\times10^{-6}$ °C$^{-1}$ [23].

The structure of the thin-walled part used in the simulation was a ring with diameter of 756 mm, which was composed of a mounting edge manufactured by forging and machining, a cold-formed ring part, and thirteen mounting seats. The thin-walled part was formed by welding of one long ring weld and thirteen short ring welds, as shown in Fig. 1. The thicknesses of the mounting edge and the ring part were both 1.3 mm. All parts were welded by manual argon arc welding and connected by I-type joints. The distribution of welds is also shown in Fig.1.

## 2 Model Establishment

### 2.1 Heat source simulation

The heat source models of welding simulation included the Gaussian analytical and double ellipsoid heat source models. This simulation adopted the double ellipsoid heat source model[24–25], as shown in Fig. 2[26]. The temperature might abruptly change at the front of the welding pool and slowly change in the rear region of welding pool, which was sufficiently considered in the double ellipsoid heat source model. Besides, the calculation results of the double ellipsoid heat source model were quite accurate. The heat distribution functions at the front and rear regions of the welding pool are as follows:

$$Q(x,y,z) = Q_f \exp\left[-\left(\frac{x^2}{a_f^2}+\frac{y^2}{b^2}+\frac{z^2}{c^2}\right)\right] \quad (1)$$

$$Q(x,y,z) = Q_r \exp\left[-\left(\frac{x^2}{a_r^2}+\frac{y^2}{b^2}+\frac{z^2}{c^2}\right)\right] \quad (2)$$

where $Q_f$ is front ellipsoid energy input (J/mm); $Q_r$ is rear ellipsoid heat input (J/mm); $a_f$ is front ellipsoid length (mm); $a_r$ is rear ellipsoid length (mm); $b$ is affected weld width (mm); $c$ is affected penetration (mm).

### 2.2 Grid division

The shell element simulation was adopted due to the thin thickness of the part used in this simulation. The amount of mesh was 43 824, and the grid unit of the weld position was 2. The schematic diagrams of mesh division and detailed partial view of the parts are shown in Fig.3.

## 3 Welding Parameters

The main influence factors related to welding quality are welding method, joint form, welding line energy, fixture, and welding sequence. The welding methods and welding parameters have a crucial influence on the welding quality, and therefore the optimization of welding parameters can effectively control welding deformation and residual stress.

**Table 1 Chemical composition of TC4 titanium alloy (wt%)[23]**

| Al | V | C | Fe | Ti |
|---|---|---|---|---|
| 5.5–6.8 | 3.5–4.5 | ≤0.1 | ≤0.3 | Bal. |

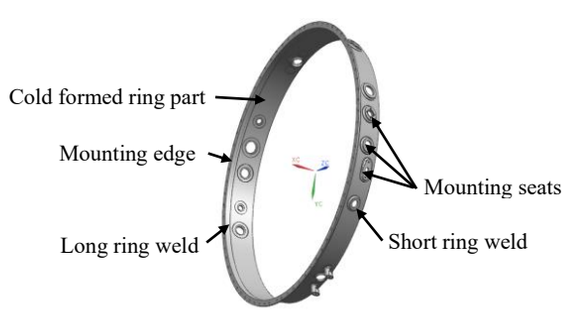


Fig.1 Schematic diagram of thin-walled part and weld distribution

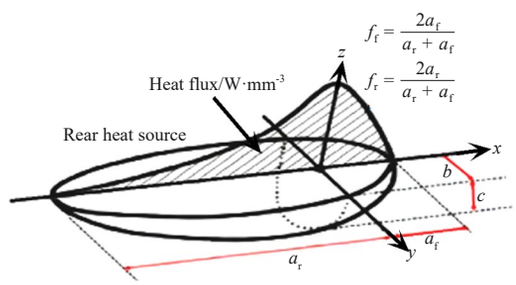


Fig.2 Schematic diagram of double ellipsoidal heat source model[26]

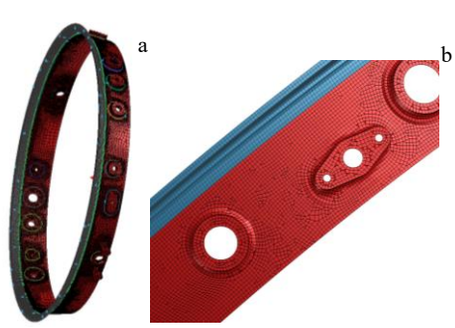


Fig.3 Schematic diagrams of mesh division (a) and detailed partial view (b) of thin-walled part

### 3.1 Welding line energy

Welding line energy directly affects the plastic deformation area, which influences the deformation and internal stress of the thin-walled part. The line energy $E=UI/v$ ($E$: line energy, J·mm$^{-1}$; $U$: voltage, kV; $I$: welding current, mA; $v$: welding speed, mm·s$^{-1}$) is mainly controlled by the welding current and welding speed. The welding line energy used in this simulation was 220, 310, and 450 J/mm.

### 3.2 Welding sequence

Because there were fourteen welds in this simulation, the quality of thin-walled parts was greatly affected by the welding sequence. In order to investigate the effects of different welding sequences on deformation and internal stress, two welding sequences were selected in this simulation. One was sequential welding: the long girth welding between the mounting edge and the cold-formed ring was conducted firstly, and then the welding of the mounting seat was conducted sequentially, as shown in Fig.4a. The other was the symmetric welding: the long girth welding between the mounting edge and the cold-formed ring was conducted firstly, and then the mounting seat was conducted in a symmetrical order, as shown in Fig.4b.

### 3.3 Fixture constraint

The application of fixtures could effectively reduce the welding deformation, whereas the residual stress of the thin-walled parts after welding would be increased due to the rigid fixation of fixtures. In order to study the influence of different fixture constraints on the deformation and residual stress, three constraint modes were selected in this simulation: gravity constraint, internal tension constraint, and internal tension+fixed mounting seats by pins. The gravity constraint indicated that no fixture was added, and the part was only constrained by the gravity, as shown in Fig. 5a. The internal tension constraint indicated that the mounting edge and cold-formed ring were internally tightened, which were equivalent to the state of fixing the mounting edge and cold-formed ring in $X$, $Y$, and $Z$ directions, as shown in Fig.5b. The constraint of internal tension+fixed mounting seats by pins indicated that the mounting edge and cold-formed ring were internally tightened, and the inner hole of each mounting seat was fixed by pins. This constraint was equivalent to state of fixing the mounting edge, cold-formed ring, and mounting seat in $X$, $Y$, and $Z$ directions, as shown in Fig.5c.

The influence of welding line energy, welding sequence, and fixture constraints on the welding temperature field, residual stress, and deformation of the thin-walled part was investigated under the abovementioned conditions. The welding parameters used in the simulation are shown in Table 2.

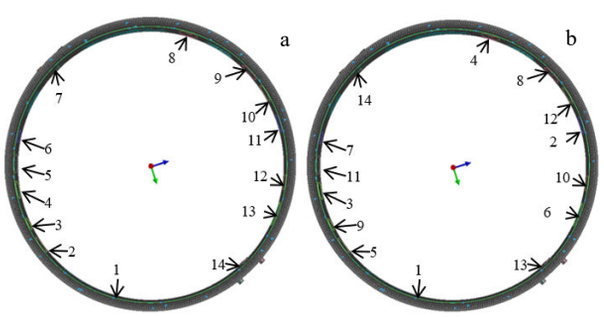


Fig.4 Schematic diagrams of sequential welding (a) and symmetrical welding (b)

## 4 Analysis and Discussion

### 4.1 Temperature field analysis

To investigate the influence of different heat inputs on the welding process and the post-weld state of the thin-walled parts, the welding processes with different line energies (220, 310, and 450 J/mm) and different thermal cycle curves were


Fig.5 Schematic diagrams of different fixture constraints on thin-walled parts: (a) gravity constraint, (b) internal tension constraint, and (c) internal tension+fixed mounting seats by pins

**Table 2 Welding parameters used in simulation**

| State | Joint form | Welding method | Line energy/ J·mm$^{-1}$ | Welding speed/mm·s$^{-1}$ | Thermal efficiency | Fixture constraint | Welding sequence |
|---|---|---|---|---|---|---|---|
| A# | I-type | Manual argon arc | 220 | 3.5 | 0.6 | Gravity | Symmetrical welding |
| B# | | | 310 | | | Gravity | Symmetrical welding |
| C# | | | 450 | | | Gravity | Symmetrical welding |
| D# | | | 310 | | | Internal tension | Symmetrical welding |
| E# | | | 310 | | | Internal tension+fixed mounting seats by pins | Symmetrical welding |
| F# | | | 310 | | | Gravity | Sequential welding |

simulated.

The melting temperature of TC4 titanium alloy is 1630–1650 °C, and the vaporization temperature of pure titanium is 3287 °C. In this simulation, the point directly below the arc was selected as the temperature measurement point. With the welding proceeding, the welding temperature rises sharply to the melting temperature. Fig. 6 shows the variation curves of welding pool temperature under different line energies. It can be seen from Fig. 6a that when the line energy is 220 J/mm, the maximum temperature of the molten pool is only 1692 °C. The width of the molten pool is small under this line energy condition, and it is difficult to completely penetrate the thin-walled part. Obviously, the heat input is too small under this line energy condition. According to Fig. 6c, when the line energy is 450 J/mm, the maximum temperature of the molten pool is 3496 °C, reaching the vaporization temperature of the pure titanium, which leads to serious burn through of the thin-walled parts. This result indicates that the line energy of 450 J/mm is too large. When the line energy is 310 J/cm, the maximum temperature of the molten pool is 2878 °C, which is between the melting and vaporization temperatures of the titanium alloy, as shown in Fig.6b. Fig. 7 shows that when the line energy is 310 J/mm, the width of the molten pool is reasonable of 7.0–8.5 mm. Therefore, the line energy of 310 J/mm is optimal.

### 4.2 Deformation

#### 4.2.1 Influence of line energy on deformation

Welding heat input depends on the line energy. The higher the heat input, the larger the plastic deformation area, and the higher the deformation degree. In this simulation, the welding processes with different line energies (220, 310, and 450 J/mm) and fixed welding sequence, fixture constraint, and other parameters were conducted. The influence of heat input change on welding deformation was analyzed, and the simulation result is shown in Fig.8.

It can be seen that the distributions of welding deformation under different line energies are basically the same. The deformation is concentrated in the areas with dense welds, and the part surface is wavy. When the line energy is 220, 310, and 450 J/mm, the maximum deformation is 5.61, 5.99, and 8.51 mm, respectively, indicating that the welding deformation is increased exponentially with increasing the line energy, as shown in Fig. 8d. According to Ref. [27], when the welding line energy reduces by 126.7 J/mm, the welding deformation reduces by 7.134 mm. Therefore, a smaller line energy input can effectively reduce the welding deformation in the welding process. Thus, it is necessary to comprehensively consider the welding deformation and weld penetration for welding heat input selection[27].

#### 4.2.2 Influence of welding constraints on deformation

The welding deformation can be effectively controlled by the welding fixture. In order to investigate the influence of fixture constraints on welding deformation, different fixture constraints (gravity, internal tension, and internal tension+fixed mounting seats by pins) were used with line energy of 310 J/mm. The welding sequence was symmetrical welding. The influence results of fixture constraints on welding deformation are shown in Fig.9.

It can be seen that the deformation distributions under different fixture constraints are quite different. The maximum deformation under gravity constraint, internal tension constraint, and constraint of internal tension+fixed mounting seats by pins is 5.99, 3.47, and 3.59 mm, respectively. Under the gravity constraint, both the deformation area and degree are more than those under other fixture constraints. Compared

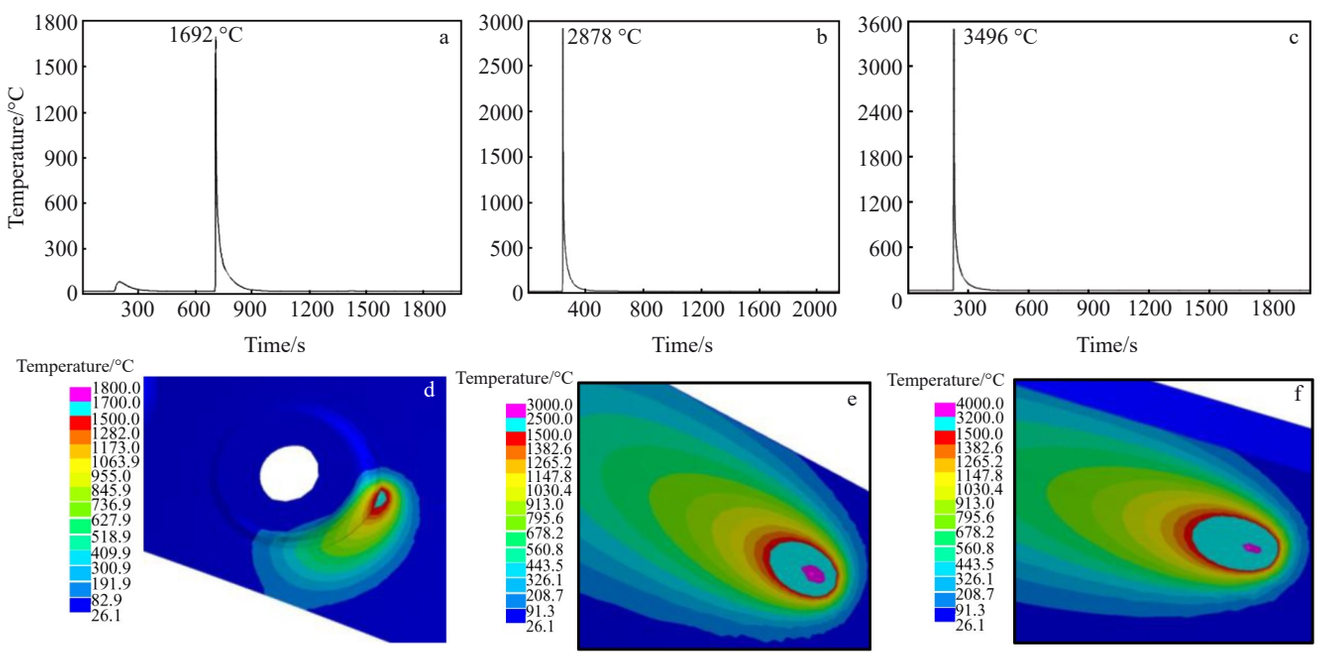


Fig.6 Welding pool temperature curves (a–c) and distributions (d–f) at line energies of 220 J/mm (a, d), 310 J/mm (b, e), and 450 J/mm (c, f)

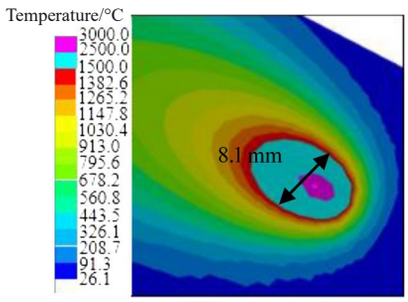


Fig.7 Simulated molten pool width under line energy of 310 J/mm

with those under the internal tension constraint, the addition of pin fixing in constraint can significantly reduce the deformation distribution area, but the maximum deformation is increased slightly. Chen et al[28] also added the welding constraints to control the welding deformation of the complex welding structures. Briefly, the optimal fixture constraint should reduce the deformation degree and deformation area as much as possible.

4.2.3 Influence of welding sequence on deformation

It is a common method to reduce the welding deformation and internal stress by adjusting the welding sequence. Generally, the welding deformation produced by symmetric welding is smaller than that by other welding sequences. To investigate the influence of welding sequence on welding deformation, the symmetrical welding and sequential welding were used in the simulation, and the simulation results are shown in Fig.10.

The maximum deformation of thin-walled parts after symmetric welding and sequential welding is 5.99 and 7.08 mm, respectively, indicating that the welding sequence has an obvious influence on the welding deformation. Thus, the influence of welding sequence on the welding deformation of

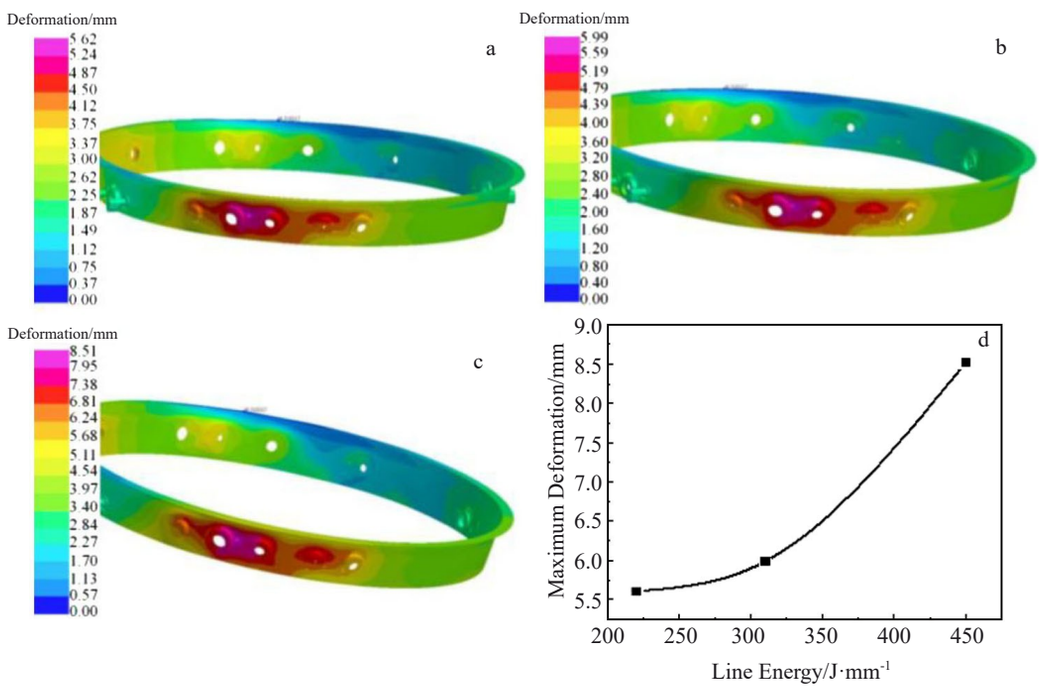


Fig.8 Deformation distributions of thin-walled parts after welding under line energies of 220 J/mm (a), 310 J/mm (b), and 450 J/mm (c); variation of deformation under different line energies (d)

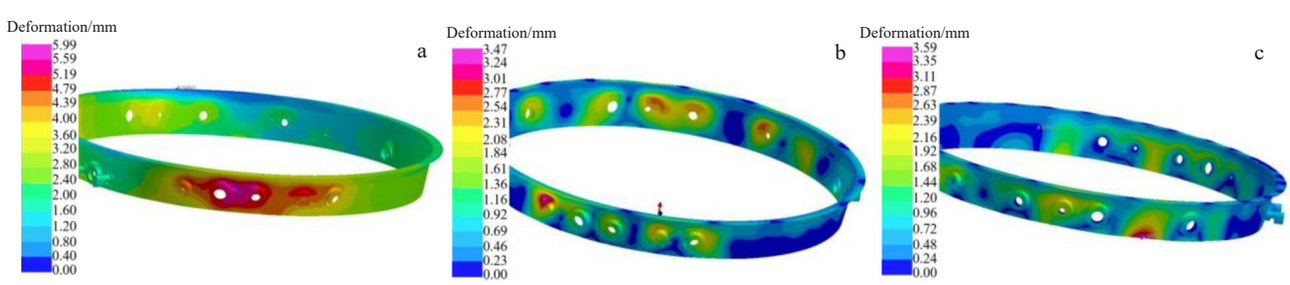


Fig.9 Deformation distributions of thin-walled parts after welding under fixture constraints of gravity (a), internal tension (b), and internal tension+fixed mounting seats by pins (c)

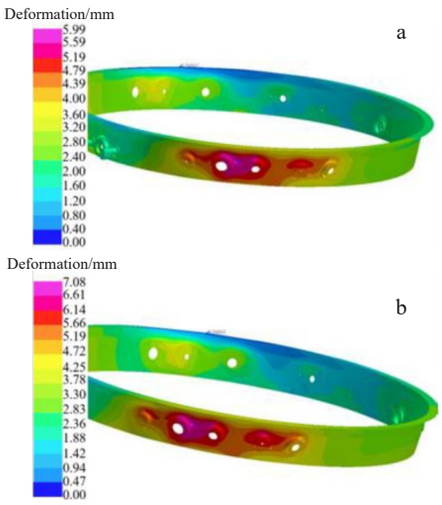


Fig.10 Deformation distributions of thin-walled parts welded in symmetric welding sequence (a) and sequential welding sequence (b)

thin-walled parts with multiple-welds should be considered in the welding process design.

### 4.3 Residual stress

During the welding process, the residual stress is inevitably caused by the plastic and elastic deformation. Residual tensile stress is one of the main factors causing hydrogen embrittlement, which significantly reduces the tensile strength of materials. The cracks are easily initiated and expand to the areas with larger residual tensile stress. The fragile position of the thin-walled part and the need of post-weld heat treatment can be determined by simulation and analysis of the residual stress distribution. The influence of line energy and fixture constraints on residual stress was investigated in this simulation.

#### 4.3.1 Influence of line energy on residual stress

The influence of line energies (220, 310, and 450 J/mm) on the distribution of residual welding stress without fixture constraints was investigated, and the results are shown in Fig.11.

The maximum residual stresses obtained under the line energy of 220, 310, and 450 J/mm are 792, 793, and 803 MPa, respectively. It can be seen that the line energy has slight effect on the residual stress. This is because the internal stress can be fully released when the welding is conducted without external constraints. The residual stress is increased slightly with increasing the line energy, and the residual stress is mainly distributed in the weld and heat-affected zone. Zeng et al[29] used the ABAQUS software to simulate the welding of 12MnNiVR alloy. When the line energy increases from 218 J/mm to 291 J/mm, the transverse residual stress increases by 44 MPa, and the longitudinal residual stress decreases by 25 MPa. Thus, with increasing the line energy, the residual stress is increased slightly.

#### 4.3.2 Influence of fixture constraints on residual stress

The effect of fixture constraints (gravity, internal tension, and internal tension+fixed mounting seats by pins) on the residual stress distribution was studied in this simulation. The results are shown in Fig.12.

Compared with that under the gravity constraint, the stress distribution area is obviously larger under other constraints. The maximum residual stress under gravity constraint,

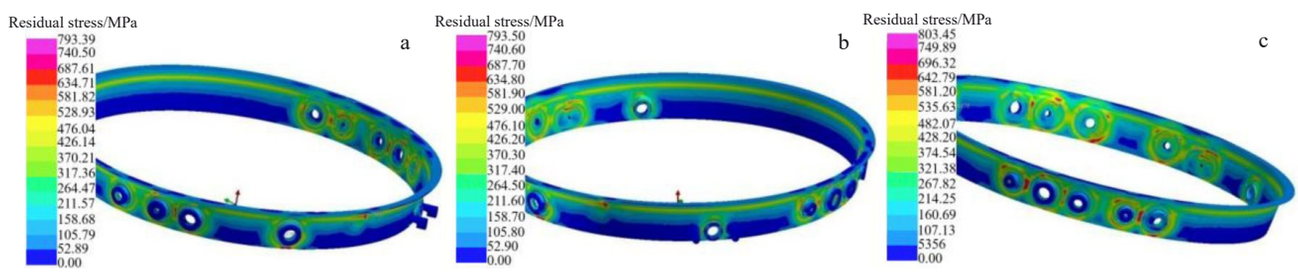


Fig.11 Residual stress distributions of thin-walled parts after welding without fixture constraint under line energies of 220 J/mm (a), 310 J/mm (b), and 450 J/mm (c)

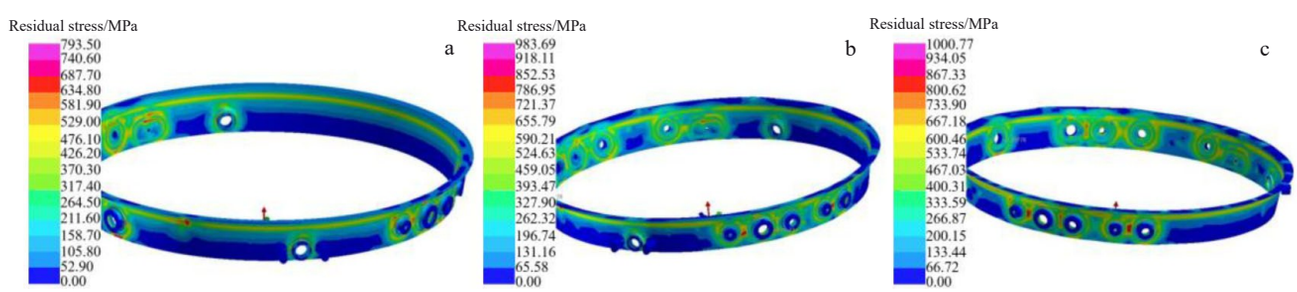


Fig.12 Residual stress distributions of thin-walled parts after welding under fixture constraints of gravity constraint (a), internal tension (b), and internal tension+fixed mounting seats by pins (c)

internal tension constraint, and constraint of internal tension+ fixed mounting seats by pins is 793, 984, and 1001 MPa, respectively. The welding deformation can be reduced by adding fixture constraints. However, due to the rigid fixation, the internal stress of the welding cannot be released freely, which significantly increases the residual stress in the clamping position. Thus, the peak stress occurs in the clamping position with a high risk of cracking.

## 5 Conclusions

1) The argon arc welding process of large-scale thin-walled and multi-welded parts used in aeroengines was simulated by the transient method. Under the optimal line energy of 310 J/mm, the width of molten pool is 7.0 – 8.5 mm, and the maximum temperature of the molten pool is 2878 °C.

2) The welding deformation is increased exponentially with increasing the line energy. Under the gravity constraint, when the line energy is 220, 310, and 450 J/m, the maximum deformation is 5.61, 5.99, and 8.51 mm, respectively. By compressing the arc during welding, the weld heat input and width can be reduced, which effectively reduces the welding deformation. Moreover, it is necessary to comprehensively consider the welding deformation and weld penetration for the selection of welding heat input.

3) The welding deformation can be effectively reduced by the fixture constraints and the maximum deformation is reduced from 5.99 mm to 3.47 mm by changing the fixture constraint from gravity to internal tension.

4) The maximum deformation of thin-walled parts after sequential welding and symmetrical welding is 7.08 and 5.99 mm, respectively. The welding sequence has a significant effect on welding deformation. The symmetrical welding method can reduce the overall deformation of the parts with multiple welds.

5) The change of welding heat input has slight effect on welding residual stress under the gravity constraint. With the addition of fixture constraint, the residual stress becomes larger, and the distribution area is expanded. The maximum residual stress is 1001 MPa under the constraint of internal tension+fixed mounting seats by pins, which results in a great risk of cracking, and the post-weld heat treatment should be conducted in time.

## References


1 Huang Liang. *The Technology and Residual Stress Analysis of Laser Welding of TC4 Titanium Alloy*[D]. Wuhan: Wuhan University of Technology, 2014 (in Chinese)

2 Tan C L, Weng F, Sui S *et al*. *International Journal of Machine Tools and Manufacture*[J], 2021, 170: 103 804

3 Wang Wen, Li Yao, Wang Qingjuan *et al*. *Rare Metal Materials and Engineering*[J], 2014, 43(5): 1143 (in Chinese)

4 Wang Shiqing, Jiao Yingxiang. *Rare Metal Materials and Engineering*[J], 2022, 51(7): 2716 (in Chinese)

5 Wu Zegang, Liu Liangbao, Sun Jianfei *et al*. *Aeronautical Manufacturing Technology*[J], 2017(21): 62 (in Chinese)

6 Hemmesi K, Farajian M, Fatemi A. *International Journal of Fatigue*[J], 2017, 101(2): 271

7 Benallal A, Billardon R, Lemaitre J. *Computer Methods in Applied Mechanics Engineering*[J], 1991, 92(2): 55

8 Prabakaran S T, Sakthivel P, Shanmugam M *et al*. *Materials Today: Proceedings*[J], 2021, 37(2): 1917

9 Wu Guodong, Shen Jingfang, Ni Dengta *et al*. *Welding Technology*[J], 2021, 50(7): 71 (in Chinese)

10 Li Xiaodong, Li Chunguang, Zhu Zhimin *et al*. *Transactions of the China Welding Institution*[J], 2014, 35(2): 104 (in Chinese)

11 Saravanan S, Raghukandan K, Kumar G S. *Optik*[J], 2019, 180: 562

12 Anawa E M, Olabi A G. *Optics & Laser Technology*[J], 2008, 40(2): 379

13 Sivagurumanikandan N, Saravanan S, Kumar G S *et al*. *Optik*[J], 2018, 157: 833

14 Hemmesi K, Farajian M, Fatemi A. *International Journal of Fatigue*[J], 2017, 101: 271

15 Shiraiwa T, Briffod F, Enoki M. *Engineering Fracture Mechanics*[J], 2018, 198: 158

16 Liu Hang. *Aircraft Engine Mounting Frame Welding Stress Analysis Based on SYSWELD*[D]. Deyang: Civil Aviation Flight Academy of China, 2022 (in Chinese)

17 Xiong Hangfeng. *Numerical Simulation of SYSWELD Welding on the Rear Frame of Electric Pallet Forklift*[D]. Hangzhou: Zhejiang University, 2020 (in Chinese)

18 Liu Chuan, Zhang Jianxun, Niu Jing. *Rare Metal Materials and Engineering*[J], 2009, 38(8): 1317 (in Chinese)

19 Ramos H M E, Tavares S M O, De Castro P. *Science and Technology of Materials*[J], 2018, 30: 6

20 Li Yana, Xie Suming, Yao Wenzhong. *Journal of Mechanical Engineering*[J], 2014, 50(8): 40 (in Chinese)

21 Xue Zhongming. *Transactions of the China Welding Institution* [J], 2003, 24(3): 87 (in Chinese)

22 Wang Jianhua. *Welding & Joining*[J], 2001(9): 5 (in Chinese)

23 Yan Minggao, Liu Bocao, Zhao Jin *et al*. *China Aeronautical Materials Handboook*[M]. Beijing: Standards Press of China, 2002, 4: 104 (in Chinese)

24 Goldak J, Chakravarti A, Bibby M. *Metallurgical Transactions* [J], 1984. 15(2): 299

25 Tsirkas S A. *Optics & Laser Technology*[J], 2018, 100: 45

26 Lee S H, Kim E S, Park J Y *et al*. *Journal of Computational Design and Engineering*[J], 2018, 5(4): 382

27 Liu Xixia. *Study on the Control of Laser Welding Deformation of Titanium Alloy Thin Sheet*[D]. Changsha: Hunan University, 2014 (in Chinese)

28 Chen Zhengxin. *Electric Welding Machine*[J], 2021, 51(12): 56 (in Chinese)

29 Zeng Zhong, Cao Jun, Zhao Jianping. *Hot Working Technology*[J], 2016, 45(5): 180 (in Chinese)

# TC4薄壁件氩弧焊焊接残余应力及变形的数值模拟

武国栋[1]，申静芳[2]，张文静[2]，谢少鹏[1]，方志忠[3]，黄晓阿[1]
(1. 广东工业大学，广东 揭阳 522000)
(2. 广东以色列理工学院，广东 汕头 515063)
(3. 中国航发贵州黎阳航空动力有限公司，贵州 贵阳 550000)

**摘　要：**基于SYSWELD专业焊接仿真软件，利用瞬态法对航空发动机TC4大型薄壁、多焊缝零件氩弧焊过程进行了数值模拟，分析了焊接线能量、夹具约束状态、焊接顺序3个因素对焊接温度场、焊接变形、残余应力的影响。结果表明：焊接变形随着线能量的增加呈指数增长；适宜的氩弧焊焊接线能量为310 J/mm；使用焊接工装约束可以有效减少焊接变形，但会导致焊接残余应力变大且残余应力分布区域更大；采用分散对称焊接的顺序焊接多焊缝零件可以降低零件整体变形。

**关键词：**TC4；数值模拟；氩弧焊

---

作者简介：武国栋，男，1992年生，硕士，广东工业大学，广东 揭阳 522000，E-mail：WGD@gdut.edu.cn